The Astrophysical Journal, 699:31–39, 2009 July 1 doi:10.1088/0004-637X/699/1/31

FERMI DISCOVERY OF GAMMA-RAY EMISSION FROM NGC 1275

A. A. Abdo[1,60], M. Ackermann[2], M. Ajello[2], K. Asano[3], L. Baldini[4], J. Ballet[5], G. Barbiellini[6,7], D. Bastieri[8,9], B. M. Baughman[10], K. Bechtol[2], R. Bellazzini[4], R. D. Blandford[2], E. D. Bloom[2], E. Bonamente[11,12], A. W. Borgland[2], J. Bregeon[4], A. Brez[4], M. Brigida[13,14], P. Bruel[15], T. H. Burnett[16], G. A. Caliandro[13,14], R. A. Cameron[2], P. A. Caraveo[17], J. M. Casandjian[5], E. Cavazzuti[18], C. Cecchi[11,12], A. Celotti[19], A. Chekhtman[20,1], C. C. Cheung[21], J. Chiang[2], S. Ciprini[11,12], R. Claus[2], J. Cohen-Tanugi[22], S. Colafrancesco[18], L. R. Cominsky[23], J. Conrad[24,25,26,61], L. Costamante[2], C. D. Dermer[1], A. de Angelis[27], F. de Palma[13,14], S. W. Digel[2], D. Donato[21], E. do Couto e Silva[2], P. S. Drell[2], R. Dubois[2], D. Dumora[28,29], C. Farnier[22], C. Favuzzi[13,14], J. Finke[1,60], W. B. Focke[2], M. Frailis[27], Y. Fukazawa[30], S. Funk[2], P. Fusco[13,14], F. Gargano[14], M. Georganopoulos[31], S. Germani[11,12], B. Giebels[15], N. Giglietto[13,14], F. Giordano[13,14], T. Glanzman[2], I. A. Grenier[5], M.-H. Grondin[28,29], J. E. Grove[1], L. Guillemot[28,29], S. Guiriec[32], Y. Hanabata[30], A. K. Harding[21], R. C. Hartman[21], M. Hayashida[2], E. Hays[21], R. E. Hughes[10], G. Jóhannesson[2], A. S. Johnson[2], R. P. Johnson[33], W. N. Johnson[1], M. Kadler[34,35,36,37], T. Kamae[2], Y. Kanai[38], H. Katagiri[30], J. Kataoka[39,62], N. Kawai[40,38], M. Kerr[16], J. Knödlseder[41], F. Kuehn[10], M. Kuss[4], L. Latronico[4], M. Lemoine-Goumard[28,29], F. Longo[6,7], F. Loparco[13,14], B. Lott[28,29], M. N. Lovellette[1], P. Lubrano[11,12], G. M. Madejski[2], A. Makeev[20,1], M. N. Mazziotta[14], J. E. McEnery[21], C. Meurer[24,26], P. F. Michelson[2], W. Mitthumsiri[2], T. Mizuno[30], A. A. Moiseev[35,42], C. Monte[13,14], M. E. Monzani[2], A. Morselli[43], I. V. Moskalenko[2], S. Murgia[2], T. Nakamori[38], P. L. Nolan[2], J. P. Norris[44], E. Nuss[22], T. Ohsugi[30], N. Omodei[4], E. Orlando[45], J. F. Ormes[44], D. Paneque[2], J. H. Panetta[2], D. Parent[28,29], M. Pepe[11,12], M. Pesce-Rollins[4], F. Piron[22], T. A. Porter[33], S. Rainò[13,14], M. Razzano[4], A. Reimer[2], O. Reimer[2], T. Reposeur[28,29], S. Ritz[21,42], A. Y. Rodriguez[45], R. W. Romani[2], F. Ryde[24,25], H. F.-W. Sadrozinski[33], R. Sambruna[21], D. Sanchez[15], A. Sander[10], R. Sato[46], P. M. Saz Parkinson[33], C. Sgrò[4], D. A. Smith[28,29], P. D. Smith[10], G. Spandre[4], P. Spinelli[13,14], J.-L. Starck[5], M. S. Strickman[1], A. W. Strong[45], D. J. Suson[47], H. Tajima[2], H. Takahashi[30], T. Takahashi[46], T. Tanaka[2], G. B. Taylor[48], J. G. Thayer[2], D. J. Thompson[21], D. F. Torres[49,50], G. Tosti[11,12], Y. Uchiyama[2], T. L. Usher[2], N. Vilchez[41], V. Vitale[43,51], A. P. Waite[2], K. S. Wood[1], T. Ylinen[52,24,25], M. Ziegler[33], H. D. Aller[53], M. F. Aller[53], K. I. Kellermann[54], Y. Y. Kovalev[55,56], Yu. A. Kovalev[55], M. L. Lister[57], and A. B. Pushkarev[58,56,59]

[1] Space Science Division, Naval Research Laboratory, Washington, DC 20375, USA
[2] W. W. Hansen Experimental Physics Laboratory, Kavli Institute for Particle Astrophysics and Cosmology, Department of Physics and SLAC National Accelerator Laboratory, Stanford University, Stanford, CA 94305, USA
[3] Interactive Research Center of Science, Tokyo Institute of Technology, Meguro City, Tokyo 152-8551, Japan
[4] Istituto Nazionale di Fisica Nucleare, Sezione di Pisa, I-56127 Pisa, Italy
[5] Laboratoire AIM, CEA-IRFU/CNRS/Université Paris Diderot, Service d'Astrophysique, CEA Saclay, 91191 Gif sur Yvette, France
[6] Istituto Nazionale di Fisica Nucleare, Sezione di Trieste, I-34127 Trieste, Italy
[7] Dipartimento di Fisica, Università di Trieste, I-34127 Trieste, Italy
[8] Istituto Nazionale di Fisica Nucleare, Sezione di Padova, I-35131 Padova, Italy
[9] Dipartimento di Fisica "G. Galilei," Università di Padova, I-35131 Padova, Italy
[10] Department of Physics, Center for Cosmology and Astro-Particle Physics, The Ohio State University, Columbus, OH 43210, USA
[11] Istituto Nazionale di Fisica Nucleare, Sezione di Perugia, I-06123 Perugia, Italy
[12] Dipartimento di Fisica, Università degli Studi di Perugia, I-06123 Perugia, Italy
[13] Dipartimento di Fisica "M. Merlin" dell'Università e del Politecnico di Bari, I-70126 Bari, Italy
[14] Istituto Nazionale di Fisica Nucleare, Sezione di Bari, 70126 Bari, Italy
[15] Laboratoire Leprince-Ringuet, École polytechnique, CNRS/IN2P3, Palaiseau, France
[16] Department of Physics, University of Washington, Seattle, WA 98195-1560, USA
[17] INAF-Istituto di Astrofisica Spaziale e Fisica Cosmica, I-20133 Milano, Italy
[18] Agenzia Spaziale Italiana (ASI) Science Data Center, I-00044 Frascati (Roma), Italy
[19] Scuola Internazionale Superiore di Studi Avanzati (SISSA), 34014 Trieste, Italy
[20] George Mason University, Fairfax, VA 22030, USA
[21] NASA Goddard Space Flight Center, Greenbelt, MD 20771, USA
[22] Laboratoire de Physique Théorique et Astroparticules, Université Montpellier 2, CNRS/IN2P3, Montpellier, France
[23] Department of Physics and Astronomy, Sonoma State University, Rohnert Park, CA 94928-3609, USA
[24] The Oskar Klein Centre for Cosmo Particle Physics, AlbaNova, SE-106 91 Stockholm, Sweden
[25] Department of Physics, Royal Institute of Technology (KTH), AlbaNova, SE-106 91 Stockholm, Sweden
[26] Department of Physics, Stockholm University, AlbaNova, SE-106 91 Stockholm, Sweden
[27] Dipartimento di Fisica, Università di Udine and Istituto Nazionale di Fisica Nucleare, Sezione di Trieste, Gruppo Collegato di Udine, I-33100 Udine, Italy
[28] CNRS/IN2P3, Centre d'Études Nucléaires Bordeaux Gradignan, UMR 5797, Gradignan, 33175, France
[29] Université de Bordeaux, Centre d'Études Nucléaires Bordeaux Gradignan UMR 5797, Gradignan 33175, France
[30] Department of Physical Sciences, Hiroshima University, Higashi-Hiroshima, Hiroshima 739-8526, Japan
[31] University of Maryland, Baltimore County, Baltimore, MD 21250, USA
[32] University of Alabama in Huntsville, Huntsville, AL 35899, USA
[33] Santa Cruz Institute for Particle Physics, Department of Physics and Department of Astronomy and Astrophysics, University of California at Santa Cruz, Santa Cruz, CA 95064, USA
[34] Dr. Remeis-Sternwarte Bamberg, Sternwartstrasse 7, D-96049 Bamberg, Germany
[35] Center for Research and Exploration in Space Science and Technology (CRESST), NASA Goddard Space Flight Center, Greenbelt, MD 20771, USA
[36] Erlangen Centre for Astroparticle Physics, D-91058 Erlangen, Germany
[37] Universities Space Research Association (USRA), Columbia, MD 21044, USA
[38] Department of Physics, Tokyo Institute of Technology, Meguro City, Tokyo 152-8551, Japan
[39] Research Institute for Science and Engineering, Waseda University, 3-4-1, Okubo, Shinjuku, Tokyo, 169-8555, Japan

[40] Cosmic Radiation Laboratory, Institute of Physical and Chemical Research (RIKEN), Wako, Saitama 351-0198, Japan
[41] Centre d'Étude Spatiale des Rayonnements, CNRS/UPS, BP 44346, F-30128 Toulouse Cedex 4, France
[42] University of Maryland, College Park, MD 20742, USA
[43] Istituto Nazionale di Fisica Nucleare, Sezione di Roma "Tor Vergata," I-00133 Roma, Italy
[44] Department of Physics and Astronomy, University of Denver, Denver, CO 80208, USA
[45] Max-Planck Institut für extraterrestrische Physik, 85748 Garching, Germany
[46] Institute of Space and Astronautical Science, JAXA, 3-1-1 Yoshinodai, Sagamihara, Kanagawa 229-8510, Japan
[47] Department of Chemistry and Physics, Purdue University Calumet, Hammond, IN 46323-2094, USA
[48] University of New Mexico, MSC07 4220, Albuquerque, NM 87131, USA
[49] Institució Catalana de Recerca i Estudis Avançats (ICREA), Barcelona, Spain
[50] Institut de Ciencies de l'Espai (IEEC-CSIC), Campus UAB, 08193 Barcelona, Spain
[51] Dipartimento di Fisica, Università di Roma "Tor Vergata," I-00133 Roma, Italy
[52] School of Pure and Applied Natural Sciences, University of Kalmar, SE-391 82 Kalmar, Sweden
[53] Department of Astronomy, University of Michigan, Ann Arbor, MI 48109-1942, USA
[54] National Radio Astronomy Observatory (NRAO), Charlottesville, VA 22903, USA
[55] Astro Space Center of the Lebedev Physical Institute, 117810 Moscow, Russia
[56] Max-Planck-Institut für Radioastronomie, Auf dem Hügel 69, 53121 Bonn, Germany
[57] Department of Physics, Purdue University, West Lafayette, IN 47907, USA
[58] Crimean Astrophysical Observatory, 98409 Nauchny, Crimea, Ukraine
[59] Pulkovo Observatory, 196140 St. Petersburg, Russia
Received 2009 March 3; accepted 2009 April 20; published 2009 June 9

ABSTRACT

We report the discovery of high-energy ($E > 100$ MeV) γ-ray emission from NGC 1275, a giant elliptical galaxy lying at the center of the Perseus cluster of galaxies, based on observations made with the Large Area Telescope (LAT) of the *Fermi Gamma-ray Space Telescope*. The positional center of the γ-ray source is only $\approx 3'$ away from the NGC 1275 nucleus, well within the 95% LAT error circle of $\approx 5'$. The spatial distribution of γ-ray photons is consistent with a point source. The average flux and power-law photon index measured with the LAT from 2008 August 4 to 2008 December 5 are $F_\gamma = (2.10 \pm 0.23) \times 10^{-7}$ ph (>100 MeV) cm^{-2} s^{-1} and $\Gamma = 2.17 \pm 0.05$, respectively. The measurements are statistically consistent with constant flux during the four-month LAT observing period. Previous EGRET observations gave an upper limit of $F_\gamma < 3.72 \times 10^{-8}$ ph (>100 MeV) cm^{-2} s^{-1} to the γ-ray flux from NGC 1275. This indicates that the source is variable on timescales of years to decades, and therefore restricts the fraction of emission that can be produced in extended regions of the galaxy cluster. Contemporaneous and historical radio observations are also reported. The broadband spectrum of NGC 1275 is modeled with a simple one-zone synchrotron/synchrotron self-Compton model and a model with a decelerating jet flow.

Key words: galaxies: active – galaxies: individual (NGC 1275) – galaxies: jets – gamma rays: observations – radiation mechanisms: non-thermal

1. INTRODUCTION

The Perseus cluster[63] is the brightest cluster of galaxies in the X-ray band and has been the focus of extensive research over many years and wavelengths. The cluster hosts the giant elliptical galaxy NGC 1275 at its center. NGC 1275 has been variously classified as a Seyfert 1.5 because of its emission-line optical spectrum, where broad lines are detected (Veron-Cetty & Veron 1998), but also as a blazar due to the strong and rapid variability of the continuum emission and its polarization (e.g., Angel & Stockman 1980; see also Pronik et al. 1999). In the radio, NGC 1275 hosts the exceptionally bright radio source Perseus A, also known as 3C 84. The source 3C 84 has a strong, compact nucleus which has been studied in detail with VLBI (Vermeulen et al. 1994; Taylor & Vermeulen 1996; Walker et al. 2000; Asada et al. 2006). These observations reveal a compact core and a bowshock-like southern jet component moving steadily outwards at 0.3 mas yr^{-1} (Kellermann et al. 2004; Lister et al. 2009). The northern counterjet is also detected, though it is much less prominent due to Doppler dimming, as well as due to free–free absorption due to an intervening disk. From these observations, Walker et al. (1994) derive that the jet has an intrinsic velocity of $0.3c$–$0.5c$ oriented at an angle $\approx 30°$–$55°$ to the line of sight. Polarization has recently been detected in the southern jet (Taylor et al. 2006), suggesting increasingly strong interactions of the jet with the surrounding environment.

The radio emission continues on larger scales, and shows a clear interaction with the hot cluster gas. Observations with *ROSAT* (Böhringer et al. 1993) and later *Chandra* (Fabian et al. 2003, 2006) reveal the presence of cavities in the gas, suggesting that the jets of 3C 84 have blown multiple bubbles in the hot intracluster medium. Perseus is the nearest and best example of a prototypical "cooling core" cluster in which the radiative cooling time of the X-ray emitting gas is considerably shorter than the age of the universe. For a β-model (Cavaliere & Fusco-Femiano 1976), the core radius of the Perseus cluster is $r_c \sim 0.3$ Mpc (or $\sim 0.^\circ 3$; see, e.g., Ettori et al. 1998; Churazov et al. 2003). Heating by the central active galactic nucleus (AGN) is thought to be responsible for balancing the radiative cooling, although the exact mechanisms by which the energy is transported and dissipated are still unclear. Shocks and ripples are clearly evident in the deep *Chandra* image of Perseus, and could provide steady heating of the center of the cluster (Fabian et al. 2005, 2006). On even larger scales, Perseus is one of the few clusters exhibiting a minihalo of size

[60] National Research Council Research Associate.
[61] Royal Swedish Academy of Sciences Research Fellow, funded by a grant from the K. A. Wallenberg Foundation.
[62] Corresponding author: J. Kataoka, kataoka.jun@waseda.jp.
[63] The Perseus cluster is Abell 426 at redshift $z = 0.0179$ and luminosity distance $d_L = 75.3$ Mpc, for a Hubble constant $H_0 = 71$ km s^{-1} Mpc^{-1} in a flat universe with $\Omega_m = 0.27$, implying 21.5 kpc arcmin^{-1}.

$\sim$300 kpc seen in low-frequency radio emission (Burns 1990). This minihalo is presumed to arise from synchrotron emission from widely distributed relativistic particles and fields energized in the central regions of the cluster.

Furthermore, the Perseus cluster appears to contain a nonthermal component, namely an excess of hard X-ray emission above the thermal bremsstrahlung from the diffuse hot cluster gas. Based on a deep *Chandra* observation, the nonthermal X-ray component has been mapped over the core of the cluster and shows a morphology similar to the radio minihalo (Sanders et al. 2005; Sanders & Fabian 2007). This claim was, however, questioned on the basis of a long *XMM-Newton* exposure (Molendi & Gastaldello 2009). Above 10 keV, a hard X-ray component has been detected with *HEAO*-1 (Primini et al. 1981) and *BeppoSAX*/PDS (Nevalainen et al. 2004), although it was not detected with *Compton Gamma Ray Observatory* (*CGRO*/OSSE in the 0.05–10 MeV range (Osako et al. 1994). More recently, 10 galaxy clusters were detected in the 15–55 keV range with *Swift*/BAT (Ajello et al. 2009). Perseus is the only cluster that displays a high-energy nonthermal component up to 200 keV, but the hard tail seen in the BAT spectrum is likely due to nuclear emission from NGC 1275 rather than to nonthermal emission from the intercluster medium. This idea is supported by possible flux variations compared to past hard X-ray observations, and by the fact that the extrapolation of the BAT spectrum is in good agreement with the luminosity of the nucleus as measured with *XMM-Newton* (Churazov et al. 2003).

At higher energies, γ-ray observations toward NGC 1275 and the Perseus clusters were first reported in the 1980s by Strong & Bignami (1983). The *COS B* data, taken between 1975 and 1979 (Strong et al. 1982; Mayer-Hasselwander et al. 1982), show a γ-ray excess at the position of the galaxy, although evidence for emission *uniquely* related to NGC 1275 is ambiguous (positional uncertainties were not given for the *COS B* data). Interpreted as emission from NGC 1275, the γ-ray flux was $F_\gamma = 8.3 \times 10^{-7}$ ph($>$70 MeV) cm^{-2} s^{-1}. Further observations in the MeV–GeV range were made by *CGRO*/EGRET in the 1990s as part of a search for γ-ray emission from 58 clusters of galaxies between 1991 and 2000 (Reimer et al. 2003). No evidence was found for high-energy γ-ray emission of individual clusters, nor as a population. The 2σ upper limit for the Perseus cluster/NGC 1275 is $F_\gamma < 3.72 \times 10^{-8}$ ph ($>$100 MeV) cm^{-2} s^{-1}, which is more than an order of magnitude lower than the flux reported by *COS B*. Observations with improved sensitivity, now possible with *Fermi*, are crucial to confirm γ-ray emission from NGC 1275 and possible time variability.

There are several reasons to think that the Perseus/NGC 1275 (3C 84) system could be a γ-ray emitter. First, a few extragalactic *non*-blazar sources, namely Centaurus A, an FR I radio galaxy (Sreekumar et al. 1999), 3C 111, a broad line radio galaxy (Nandikotkur et al. 2007; Hartman et al. 2008), and possibly the radio galaxy NGC 6251 (Mukherjee et al. 2002), were already detected with EGRET. In contrast to blazars, which form the majority of extragalactic γ-ray sources (Hartman et al. 1999), most radio galaxies have large inclination angles and hence there is no significant amplification of the emission due to Doppler beaming. However, if the jet has velocity gradients (see Georganopoulos & Kazanas 2003b for a decelerating flow and Ghisellini et al. 2005 for a spine-sheath velocity profile), as suggested by recent radio/X-ray observations (e.g., for transversal profiles, see Laing & Bridle 2002; Kataoka et al. 2006), it is possible to produce bright γ-ray emission from the nuclei of some radio galaxies via the inverse Compton process where the emission from the slow part is amplified in the rest frame of the faster part, and vice versa. Second, γ-ray emission from the cluster is also expected as a result of (1) secondary nuclear interactions of high-energy cosmic rays with the intercluster medium or as the origin of a secondary population of relativistic electrons (Berezinsky et al. 1997; Atoyan & Völk 2000); (2) particle acceleration at large-scale scale shocks in forming clusters (e.g., Totani & Kitayama 2000), or at a shock excited by an AGN outburst at the cluster center (Fujita et al. 2007); and (3) dark matter annihilation, which also acts as a heat source in the core of cooling flow clusters (Totani 2004). In contrast to the emission from a compact AGN region, γ-rays from clusters would be steady on the observing time scales. Hence time variability, if detected, provides an important clue to the origin of the γ-ray emission.

With the successful launch of *Fermi* (formerly known as *GLAST*), we have a new opportunity to study γ-ray emission from radio galaxies and cluster of galaxies with much improved sensitivity. As a first step, we report here the *Fermi* discovery of γ-ray emission from NGC 1275. In Section 2, we describe the *Fermi* γ-ray observations, data reduction process, and analysis results. In Section 3, we present historical radio and contemporaneous radio observations with the UMRAO, RATAN, and the MOJAVE program. Our results are presented in the context of jet emission models in Section 4. Conclusions are given in Section 5.

2. γ-RAY OBSERVATIONS

On 2008 June 11, the *Fermi Gamma-ray Space Telescope* was successfully launched into a low-Earth orbit at $\sim$565 km, with an inclination angle of 25.°5. The Large Area Telescope (LAT) instrument on *Fermi* is described in detail in Atwood et al. (2009) and references therein. The LAT relies on the conversion of γ-rays into electron–positron pairs; tracking of those pairs allows the determination of the direction of the incident γ-ray. Such a design results in a wide field of view ($\simeq$2.4 sr), simultaneously available to the detector. Compared to earlier γ-ray missions, the LAT has a large effective area ($\sim$8000 cm^2 on axis at 1 GeV for the event class considered here), wide energy coverage from $\approx$20 MeV to $>$300 GeV, improved angular resolution (a point-spread function (PSF) of $\sim$0.°6 at 1 GeV for 68% containment) and is live about 90% of the time.

During the first year of operations, most of the telescope's time is being dedicated to "survey mode" observing, where *Fermi* points away from the Earth, and nominally rocks the spacecraft axis north and south from the orbital plane to enable monitoring of the entire sky on a timescale shorter than a day or less. The whole sky is surveyed every $\sim$3 hours (or 2 orbits). The first light images of the γ-ray sky are found in the LAT official web page.[64] We report here on the LAT's initial observations of the Perseus/NGC 1275 region, using data collected during the first four months of the ongoing all-sky survey. The source was first detected during the Launch and Early Operation phase (L&EO, namely the period lasting approximately 60 days after the launch until August 3). However, because the instrument configuration was not tuned for optimum performance, we concentrate our analysis on the survey data starting from 2008 August 4.

[64] http://www.nasa.gov/mission_pages/GLAST/main/index.html

2.1. Data Reduction

The data used here comprise all scientific data obtained between 2008 August 4 and 2008 December 5. The interval runs from MET 239557417 to 250134308. We have applied the zenith angle cut to eliminate photons from the Earth's limb, at 105°. This is important in pointed mode observations, but also important for survey mode due to overshoots and sun avoidance maneuvers. The same zenith cut is also accounted for in exposure calculation using the LAT science tool GTLTCUBE. We use the "Diffuse" class events (Atwood et al. 2009), which are those reconstructed events having the highest probability of being photons.

In the analysis presented here, we set the lower energy bound to a value of 200 MeV, since the bin count for photons with energies of ≈ 100 MeV and lower is systematically lower than expected based on extrapolation of a reasonable function. Note that theta cuts, which would eliminate events close to the edge of the field of view, are not applied in the present analysis since we still need to study the tradeoffs introduced by the cut versus those introduced by not having the cut. Science Tools version v9r8p3 and Instrumental Response Functions (IRFs) P6_V1 (a model of the spatial distribution of photon events calibrated prelaunch) were used throughout this paper.

2.2. γ-ray Results

Figure 1 shows a close-up of the *Fermi* image above 200 MeV centered on the position of NGC 1275 (R.A. = 49.°951, decl. = 41.°512), with an image radius of the Region of Interest (ROI) $r = 8$ deg. The image has been smoothed with a two-dimensional Gaussian function with $\sigma = 0.°2$. The extended feature toward the upper left is the edge of the Galactic diffuse emission. The brightest source is located at R.A. = 50.°000, decl. = 41.°524, and coincides within the uncertainties with the direction to NGC 1275. The positional center of the γ-ray emission is only 0.°05 from the position of the NGC 1275 nucleus, well within the 95% LAT error circle of 0.°086.[65]

Figure 2 shows the projection of the γ-ray images in low (0.2–1 GeV) and high (1–10 GeV) energy bands, specifically, sliced photon count distributions projected onto a R.A. axis with $\Delta\theta_{\rm decl.} = \pm 2°$, centered on NGC 1275 (black points with errors; bin width 0.°1). The most prominent peak in the center is NGC 1275, while the smaller peak is also seen in the east ("src_A"). The red solid lines show the best-fit model determined from the likelihood analysis described below, in which we assume two point sources (NGC 1275 and src_A) with the Galactic and extragalactic diffuse emission overlaid. The LAT has an angular resolution of $\theta_{68} \simeq 0.°6 E_{\rm GeV}^{-0.75}$ (Atwood et al. 2009), giving $\theta_{68} \approx 2.°0$ at 200 MeV. The counts distributions of NGC 1275 and src_A are consistent with this distribution in low- and high-energy bands, indicating that the diffuse extended component combined with a point source for src_A does not contaminate NGC 1275/Perseus, at least within current photon statistics.

To study the average spectrum of NGC 1275 during the four-month observation, we use the standard maximum-likelihood spectral estimator provided with the LAT science tools GTLIKE.

[65] More accurately, we should call this the "NGC 1275/Perseus region," since at this stage it is still unclear whether the γ-ray emission comes from the nucleus of NGC 1275 or the Perseus cluster. This will be discussed later in the discussion in Section 4. Also there are several galaxies, NGC 1273, 1274, 1277, 1278, and 1279 in the LAT error circle, but NGC 1275 is by far the brightest, is strong in the radio, and is the closest source to the γ-ray peak position.

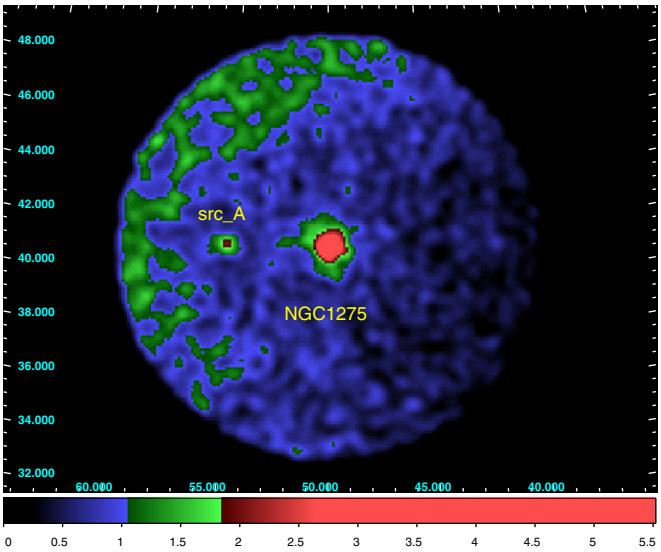

Figure 1. γ-ray sky map obtained with *Fermi* at $E > 200$ MeV, centered on NGC 1275 (image radius $r = 8°$, which is the value used throughout this paper). Sky survey data between August 4 and December 5 are accumulated. Full details are given in the text.

This fits the data to a source model, along with models for the uniform extragalactic and structured Galactic backgrounds. As shown in Figure 1, the upper left count map (≃10° from the NGC 1275 nucleus) is dominated by the bright soft γ-ray emission of the Galactic plane. Since the distribution and amount of the Galactic diffuse emission itself are still a matter of debate, careful choice of the source region is important especially for relatively faint sources. We, therefore, made several trials by changing the ROI radius from 5° to 20° in steps of 5°, 8°, 10°, 12°, 15°, and 20°, respectively.[66] We used a recent Galactic diffuse model, 54_59Xvarh7S, generated using GALPROP with the normalization free to vary in the fit. The response function used is P6_V1_DIFFUSE.

Since a different choice of ROI yielded essentially the same results within statistical uncertainties, we set $r = 8°$ in the following analysis to minimize contamination from the Galactic plane and nearby sources (for details, see the *Fermi* LAT bright γ-ray source list; Abdo et al. 2009) and to reduce computational time; this region is large enough to contain most of the photons even at the lowest energies where the LAT PSF broadens. With this choice, the only sources to be included in the modeling are NGC 1275, src_A, and the Galactic and extragalactic emission as underlying diffuse background components. We have also checked the contribution from sources outside the ROI, but found it to be completely negligible.

We model the continuum emission from both NGC 1275 and src_A with a single power law. The extragalactic background is assumed to have a power-law spectrum, with its spectral index and the normalization free to vary in the fit. From an unbinned GTLIKE fit the best-fit power-law parameters for NGC 1275 are

$$\frac{dN}{dE} = (2.45 \pm 0.26) \times 10^{-9} \times \left(\frac{E}{100\ \text{MeV}}\right)^{-2.17\pm0.04} \text{ph cm}^{-2}\ \text{s}^{-1}\ \text{MeV}^{-1}, \quad (1)$$

[66] The LAT team recommends that the ROI should be at least 15°–20° in confused regions near the Galactic plane, ⩽10° for isolated high-latitude regions.

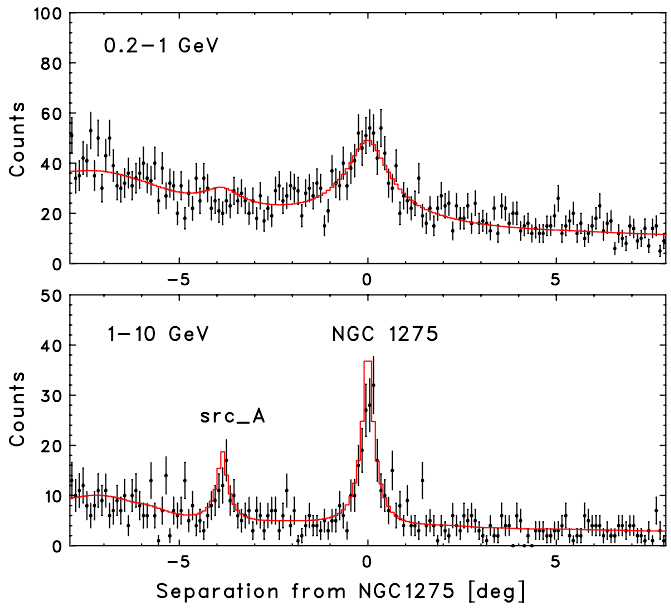

Figure 2. Comparison between data (black points) and GTLIKE model (red solid line) in low- (0.2–1 GeV; upper) and high- (1–10 GeV; lower) energy bands for sliced projected count distribution. In each energy band, γ-ray images are projected onto the x-axis (i.e., R.A. plane) with sliced declination width $\pm 2^\circ$ centered on NGC 1275. Bin width is $0.^\circ 1$.

or

$$F_\gamma = (2.10 \pm 0.23) \times 10^{-7} \mathrm{ph}(> 100\ \mathrm{MeV})\ \mathrm{cm}^{-2}\ \mathrm{s}^{-1}, \quad (2)$$

where only statistical errors are taken into account and the spectrum was extrapolated down to 100 MeV. Systematic errors for the LAT are still under investigation (P. Bruel et al. 2009, in preparation), but for a relatively faint source like NGC 1275, the uncertainty is dominated by statistical errors.

The predicted photon counts from NGC 1275 in the ROI are $N_{\mathrm{pred}} = 866.5$ and the test statistic (defined as $TS = 2(\log L - \log L_0)$, where L and L_0 are the likelihood when the source is included or not) is $TS = 1206.6$ above 200 MeV, corresponding to a 35σ detection. For the Galactic diffuse background, the normalization is 1.050 ± 0.026 and $N_{\mathrm{pred}} = 11542.8$. The near unity normalization suggests that the Galactic diffuse emission estimated in the ROI is in good agreement with the current GALPROP model. The power-law photon index of the extragalactic background is $\Gamma = 2.14 \pm 0.04$ with $N_{\mathrm{pred}} = 2793.2$. This spectral shape is consistent with what has been measured with *CGRO*/EGRET ($\Gamma = 2.10 \pm 0.03$) but the normalization determined with *Fermi*, $(1.23 \pm 0.16) \times 10^{-7}$ photons cm^{-2} s^{-1} MeV^{-1} when extrapolated to 100 MeV, is about 30% lower than that measured with EGRET (Sreekumar et al. 1998). Although we have considered src_A, the source turned out to be weak and did not affect the analysis results presented here.[67] Figure 3 shows the LAT spectrum of NGC 1275 obtained by separately running GTLIKE for seven energy bands; 200–400 MeV, 400–800 MeV, 800 MeV−1.6 GeV, 1.6–3.2 GeV, 3.2–6.4 GeV, 6.4–12.8 GeV, and 12.8–25.6 GeV, where the dotted line shows the best-fit power-law function for the NGC 1275 data given by Equation (1).

Finally, we investigate the flux variations of NGC 1275 from August 4 to December 5 in 2008. To this end, we accumulated

[67] In summary, the best-fit parameters for a power-law function gives the photon index $\Gamma = 1.92 \pm 0.20$ with $F_\gamma = (0.25 \pm 0.16) \times 10^{-7}$ph(> 100MeV)cm^{-2}s^{-1} for src_A.

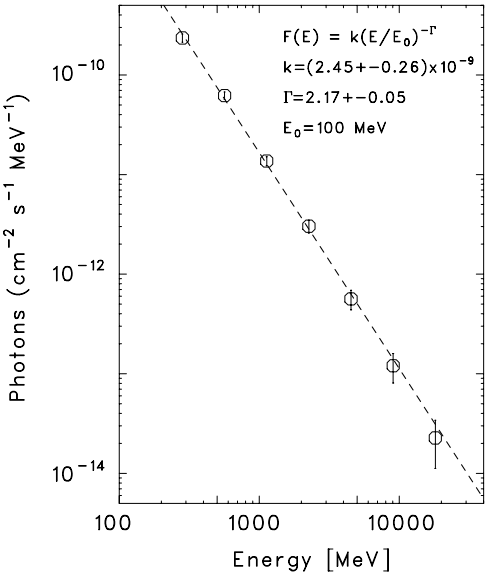

Figure 3. LAT spectrum of NGC 1275 from 200 MeV to 25 GeV (open circles). A dashed line (parameters given in the upper right of the figure) shows the best-fit power-law function determined from the GTLIKE as given in the text.

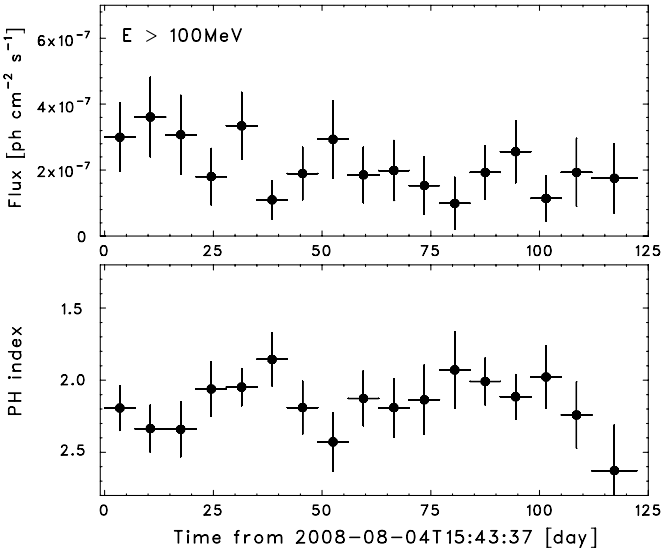

Figure 4. Temporal variation of γ-ray flux and spectral index during the 2008 August–December observation. The observation time is measured from the start of the *Fermi* observation, i.e., 2008 August 4 15:43:37 UT. Upper panel: changes in the $E > 100$ MeV fluxes (calculated from an extrapolation of $E > 200$ MeV spectrum). Lower panel: changes in the power-law photon index. Background diffuse emission (both Galactic and extragalactic) is fixed at the best-fit parameters determined from an average spectral fitting as given in the text, and only statistical errors are shown.

spectra with a time resolution of 7 days and fit each spectrum with the same model as above. The ROI radius ($r = 8^\circ$), energy range ($E > 200$ MeV), and other screening conditions were the same as described above. Since variability is *not* expected for underlying background diffuse emission, we fixed the best-fit parameters as to an average values determined from the four-month integrated spectrum for the Galactic/extragalactic background components. In this manner, only four parameters (power-law photon indices and normalizations for both NGC 1275 and src_A) are set to be free for the time-resolved spectral fits.

Figure 4 shows the plot of the flux ($E > 100$ MeV: *upper*) and photon index (*lower*) versus time. It appears that the flux

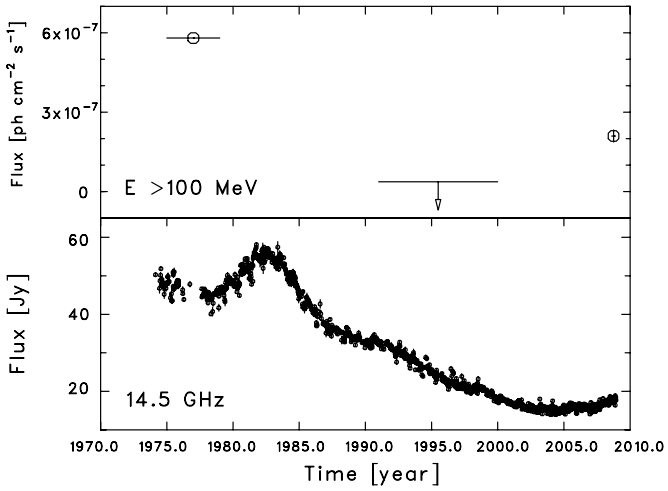

Figure 5. (Upper) Historical γ-ray activity of 3C 84 measured above 100 MeV. *COS-B* flux in this energy range was estimated by assuming a differential spectral index of $\Gamma = 2.0$. (Lower) A long-term radio light curve of 3C 84 taken with the UMRAO at 14.5 GHz between 1974 February and 2008 December. Data are binned with daily averages. The radio light curve is in a rising state during the *Fermi* observations.

of NGC 1275 may decrease gradually over four months, and there are some hints of spectral evolution as well. However, the hypothesis of constancy cannot be rejected, with $\chi^2 = 12.2$ and 12.4 for 16 degrees of freedom, for flux and photon index variations, respectively.[68] We checked that the contaminant src_A does not vary. We independently checked the light curve using GTEXPOSURE, taking a small ROI radius of $r = 2^\circ$ to reduce the contamination from diffuse background and nearby sources. We assumed the spectral photon index of $\Gamma = 2.2$, and background was subtracted from nearby region of the same ROI radius. The results were consistent with what has been obtained with GTLIKE. Further long-term monitoring of this source is important. Since the source is apparently variable on longer timescale, year-scale variability is naturally expected as we will discuss below.

3. RADIO OBSERVATIONS

In the radio, the University of Michigan Radio Astronomy Observatory (UMRAO) have monitored 3C 84 since 1965. The UMRAO variability program utilizes a 26 meter prime focus paraboloid equipped with transistor-based radiometers which operate at the central frequencies 4.8, 8.0, and 14.5 GHz; the bandwidths are 560, 760, and 1600 MHz, respectively. A typical observation consists of 8–16 individual measurements obtained over a 20–40 minute time interval. The flux scale is set by observations of Cassiopeia A (e.g., see Baars et al. 1977). Further details of the UMRAO calibration and data analysis procedures are given in Aller et al. (1985). Figure 5 shows a long-term light curve of 3C 84 measured at 14.5 GHz, taken by the UMRAO from 1974 February to 2008 December. Interestingly, the radio flux density reached a maximum between 1980 and 1985 (the *COS B* era), and then substantially faded out after 1990 (O'Dea et al. 1984; Teräsranta et al. 2004) when EGRET was observing. This trend appears similar to the optical activities of this source (Nesterov et al. 1995; Pronik et al. 1999). Furthermore, the UMRAO light curve shows a flare (or a rising state) starting in 2005, which could be interpreted as an ejection of new jet components.

In fact, the Monitoring Of Jets in Active galactic nuclei with VLBA Experiments (MOJAVE; Lister et al. 2009) 15 GHz VLBA observations of 3C 84, taken simultaneously with *Fermi* on 2008 August 25, show a significant brightening of the central sub-parsec-scale structure, indicating that a flare is happening in the innermost jet region (Figure 6). This brightening might be connected to the γ-ray activity detected. The 1–22 GHz instantaneous radio spectrum of 3C 84 was also observed with the 600 meter ring radio telescope RATAN-600 of the Special Astrophysical Observatory, Russian Academy of Sciences, located in Zelenchukskaya, Russia, on 2008 September 11 and 12. The continuum spectrum was measured on both days quasi-simultaneously (within several minutes) in a transit mode at six different bands with the following central frequencies (and frequency bandwidths): 0.95 GHz (0.03 GHz), 2.3 GHz (0.25 GHz), 4.8 GHz (0.6 GHz), 7.7 GHz (1.0 GHz), 11.2 GHz (1.4 GHz), and 21.7 GHz (2.5 GHz). Details on the method of observation, data processing, and amplitude calibration are described in Kovalev et al. (1999). An average spectrum is used for the spectral energy distribution (SED).

4. DISCUSSION AND INTERPRETATION

In the previous sections, we have reported the detection of γ-ray emission from NGC 1275 during the initial sky survey with *Fermi*, and historical and contemporaneous radio observations with UMRAO, RATAN, and MOJAVE. Although excess γ-ray emission around the position of this galaxy had been previously found with *COS B*, the association of the latter with NGC 1275 was ambiguous, due to the relatively poor angular resolution and low photon statistics (Strong & Bignami 1983; see Section 1). The *Fermi* observations, with much improved sensitivity and angular resolution, allow us to more precisely determine the localization of the γ-ray source and its possible association with NGC 1275. More intriguing is that the source was not detected during *CGRO*/EGRET observations over 10 viewing periods (Reimer et al. 2003). The 2σ EGRET upper limit to the flux is $F_\gamma < 3.72 \times 10^{-8}$ ph($>$100 MeV) cm^{-2} s^{-1}, which is about a factor of seven *lower* than the flux measured by *Fermi*/LAT, and more than an order of magnitude lower than the *COS B* flux (see Figure 2). This means the source varies on timescales shorter than years to decades, so that the emission region size $R \lesssim ct_{\rm var} \approx 0.3$ pc.

With this simple estimate, we can provide useful constraints on whether the γ-ray emission originates from a cluster or AGN. Although the LAT error circle is still large enough to include both nonthermal AGN and nonthermal cluster emission, a large fraction of the γ-ray emission measured with the *Fermi* LAT must originate from within a few light years of an active region, most likely the cluster center, on the basis of the EGRET upper limit. Since the Perseus cluster is extended over $\gtrsim 0.^\circ 5$ (or β radius $\sim 0.^\circ 3$; see Section 1), corresponding to hundreds of kpc, if the emission were extended on this size scale, it would not have been variable and could have been detected as an extended source with the LAT above 1 GeV, where the PSF becomes smaller than $\approx 0.^\circ 5$. As seen in Figure 2, however, the observed count distribution is consistent with a point source.

This limits the γ-ray flux from the cluster formed by (1) p–p interactions of high-energy cosmic rays or by (2) particle

[68] NGC 1275 is flagged as a variable source in the *Fermi* LAT bright γ-ray source list (Table 6 of Abdo et al. 2009). This is because they have fixed the spectral index of each source to the best-fit value over the full interval to avoid large error bars in the flux estimates, while both flux and photon index are free to vary in the fit of this paper. Further long-term monitoring is thus important to confirm the variability of this source.

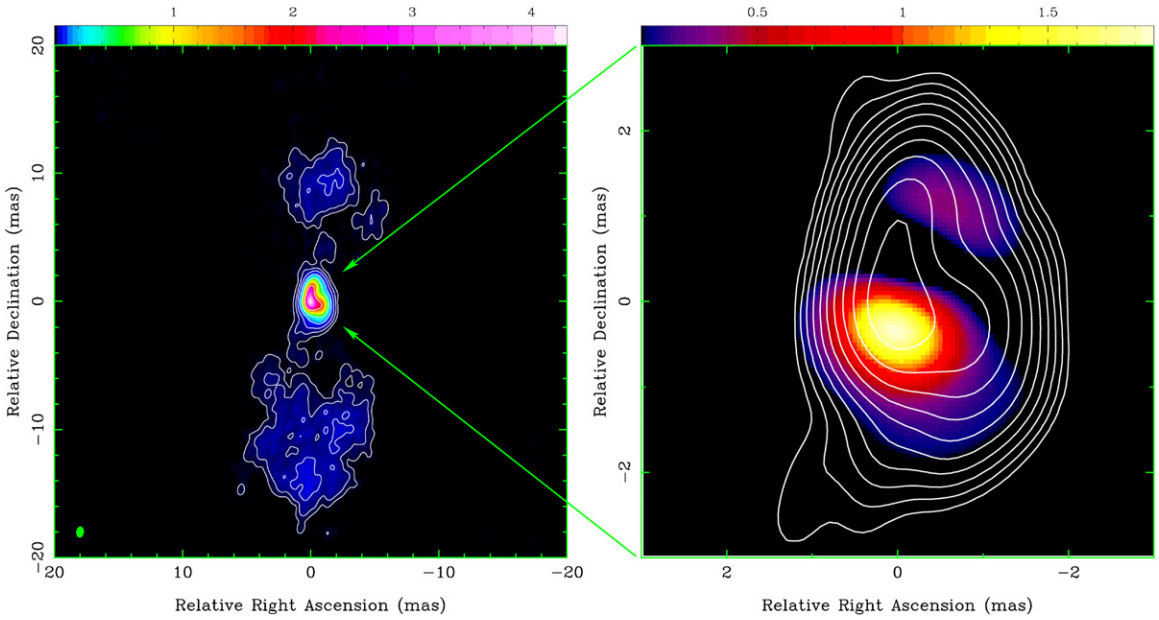

Figure 6. Left: naturally weighted VLBA Stokes I 15.3 GHz image of 3C 84 observed within the MOJAVE project (Lister et al. 2009) on 2008 August 25. It is shown both in color and in contours. The peak intensity is 4.3 Jy beam^{-1}. The beam (0.87 × 0.58 mas) is shown in the left corner (green). Right: a close-up of the central region (contours). A difference image between 2008 August 25 and 2007 September 06 is shown in color, where 1 mas circular restoring beam was used for both epochs. It clearly shows that the innermost jet region has brightened significantly, and hence a radio flare is happening during the *Fermi* observations in 2008. Units for color wedges are Jy beam^{-1}. One milliarcsecond is about 0.36 pc.

acceleration at a large-scale shock to the flux upper limit measured with EGRET (see Section 1). Thus, the bulk of the *Fermi* emission is limited to a region of a few light years in extent. One may also suspect that the high-energy γ-ray emission could be related to the "cavities" seen in the X-ray images of the Perseus Cluster (Fabian et al. 2000, 2003), which are likely inflated by the jet from 3C 84. Their size scale, on the order of arcminutes, is too large to account for the inferred time variability.

Another possibility is the γ-ray flux originates from the annihilation of dark matter particles, for example, neutralino dark matter. An annihilation γ-ray signal from the whole cluster would be extended and inconsistent with the *Fermi* observation. In any case, the expected flux is much smaller when a standard annihilation cross section is assumed. However, the growth of the supermassive black hole at the cluster center may produce a spike in the density profile, resulting in a much higher annihilation rate from the central region within ∼0.1 pc (e.g., Totani 2004; Colafrancesco et al. 2007). This annihilation emission should be observed as a point source for the LAT resolution, and flux modulation on the dynamical timescale (∼four months within 0.1 pc) is possible. However, the continuum γ-ray spectrum from neutralino annihilation should be strongly peaked at ∼1–10 GeV in the standard framework of particle physics, which conflicts with the observed LAT spectrum (Figures 3 and 2).

The available evidence appears to be most consistent with γ-ray emission arising from the pc-scale AGN jet. Nonthermal nuclear emission is also detected at other wavelengths. Recent *Chandra* and *XMM-Newton* observations with excellent angular resolution to resolve the nucleus revealed that nonthermal nucleus emission is well represented by a simple power-law function of $\Gamma = 1.65$ (Churazov et al. 2003; Balmaverde et al. 2006; Molendi & Gastaldello 2009), with some hints of flux variations. Also, hard X-ray emission detected with *Swift*/BAT is likely due to nonthermal emission from the nucleus of NGC 1275 (Ajello et al. 2009). In the optical, nuclear variability of NGC 1275 has been indicated in densely monitored observations since the 1960s (Nesterov et al. 1995; Pronik et al. 1999). The source was highly variable and bright in the 1970s ($m_R \simeq 12.0 \pm 0.5$ mag), suddenly faded in the 1980–1990s with $m_R \simeq 13.5$ mag (Ciprini et al. 2008), and has been gradually rising up again after 2000. To gauge the recent optical activity of NGC 1275, we measured the source flux in six filter *Swift*/UVOT (Roming et al. 2005) images from 2007 December (Figure 7) using $r = 5''$ circular regions. Additionally, our recent optical observations by Multicolor Imaging Telescope for Survey and Monstrous Explosions (MITSuME; e.g., Kotani et al. 2005) exhibits preliminary results of $m_R \simeq 12.7 \pm 0.3$ mag during the *Fermi*/LAT observation in 2008 June–September. Interestingly, it appears that the optical flux traces the historical γ-ray activity from *COS B* to the *Fermi* era. Note, however, that care must be taken when comparing results from different telescopes due to host galaxy subtraction and different techniques to calculate photon counts (Nilsson et al. 2007).

Figure 7 shows the overall νF_ν SED of NGC 1275 constructed with radio to γ-ray multiband data. Although the archival NASA/IPAC extragalactic database (NED) data contain host galaxies contamination in optical, the nonthermal nuclear spectrum shows two pronounced continuum components, one peaking between the optical and IR and the other in the γ-ray regime. In analogy with blazars (e.g., Kubo et al. 1998; Fossati et al. 1998), the low-energy component is probably due to synchrotron radiation of relativistic electrons accelerated within the outflow, while Compton scattering by the same electron is most likely responsible for the nonthermal X-ray and high-energy γ-ray component. As can be seen, the γ-ray flux is comparable in apparent luminosity with the lower energy radio/optical flux. Hence the overall SED appears to be similar to low-frequency-peaked BL Lac objects (e.g., Kubo et al. 1998) in that the low-energy peak is in the IR–optical and the high peak is in the soft γ-rays. Two low-peaked BL Lacs have been observed with TeV

γ-rays: BL Lac (Albert et al. 2007) and 3C 66A (Acciari et al. 2009), and thus NGC 1275 is a potential TeV source as well.

We use two models to fit the SED of the nonthermal emission of NGC 1275 in Figure 7. First, we consider a simple one-zone synchrotron self-Compton (SSC) model fit to the *Fermi* data and contemporaneous radio data (blue dashed curve; see Finke et al. 2008 for details). This model employs a jetted outflow with bulk Lorentz factor $\Gamma = 1.8$ and Doppler factor $\delta = 2.3$, so that the observing angle to the jet direction is $\theta = 25^\circ$. The mean magnetic field in the radiating plasma is $B = 0.05$ G, and the comoving radius of the jet emission region is 2×10^{18} cm, corresponding to a variability timescale of ≈ 1 yr. The nonthermal electron distribution is assumed to be described by a broken power law with number indices (where the electron distribution $n(\gamma) \propto \gamma^{-p}$) $p_1 = 2.1$ for $800 \lesssim \gamma \leqslant 960$, and index $p_2 = 3.1$ for $960 \leqslant \gamma \leqslant 4\times10^5$, where γ is the electron Lorentz factor in the fluid frame, and the Poynting flux density is about twice the electron energy density. This simple homogeneous model provides an adequate fit to the NGC 1275 data, and is consistent with mildly relativistic outflows observed in the expanding radio lobe of 3C 84 (Asada et al. 2006). An apparent discrepancy between the model and data in optical–UV emission can be accommodated by the remaining host galaxy contribution as described above.

In the standard blast wave scenario, the jet protons will contain the majority of the jet's kinetic energy, and will be radiatively inefficient since they are unlikely to lose their energy without a significant observable component. If we assume they have 10 times the energy density of the electrons, the total jet power will be 2.3×10^{45} erg s^{-1}, which may be inconsistent with the estimated power required to inflate the lobe of 3C 84 against the pressure of the hot cluster gas, $(0.3\text{–}1.3)\times10^{44}$ erg s^{-1} (Dunn & Fabian 2004), although the jet power in the past could be lower than at present. With the assumption that there is one cold proton in the flow for each radiating electron, we will get a total jet power of 3.8×10^{44} erg s^{-1}, which is consistent to within a factor of 2 of the lobe inflation power. Furthermore, in the context of BL Lac and FR I unification, larger values of Γ near the base of the jet are expected if NGC 1275 is a misaligned BL Lac object. Velocity gradients in the jet also help to resolve spectral modeling issues in BL Lac objects (Georganopoulos & Kazanas 2003b; Ghisellini et al. 2005) and the apparent conflict between the subluminal VLBI apparent speeds usually measured in TeV BL Lacs (e.g., Piner et al. 2008) and the need for highly relativistic outflows required to model their TeV emission.

A fit to the NGC 1275 data using the decelerating flow model of Georganopoulos & Kazanas (2003b), which was developed to overcome these problems, is also shown in Figure 7 (blue solid curve). In this model, the high-energy emission is due to synchrotron photons produced in the slower part of the flow that are Compton-scattered by energetic electrons in the faster, upstream part of the flow (Georganopoulos & Kazanas 2003a). The jet starts with a bulk Lorentz factor $\Gamma_{\rm max} = 10$ and decelerates down to $\Gamma_{\rm min} = 2$ over a distance of 5×10^{17} cm. The cross section of the flow at the inlet has a diameter of 3×10^{16} cm, and the magnetic field at the base is $B = 0.2$ G. The injected power-law electron distribution, $n(\gamma) \propto \gamma^{-p}$ has an index $p = 1.8$, and extends from $\gamma_{\rm min} = 800$ to $\gamma_{\rm max} = 1.0\times10^5$, and the particle energy density is higher than the magnetic field energy density by a factor of 13. If the protons have 10 times the energy density of the electrons, the total jet power is $L_{\rm jet} = 4.9\times10^{44}$ erg s^{-1}, which is still above the power needed to inflate the lobes. With an assumption of one proton per radiating electron, the total jet power, $L_{\rm jet} = 6.0\times10^{43}$ erg s^{-1}, is consistent with this value.

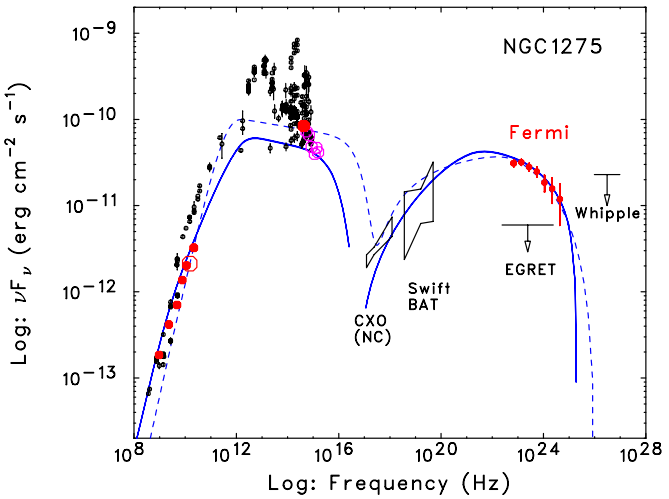

Figure 7. Overall SED of NGC 1275 constructed with multiband data, using radio (RATAN-600 in filled red circle; this work), radio core (MOJAVE in open red circle; this work), optical (MITSuME in red; this work), optical/UV (*Swift*/UVOT in open magenta circle; this work), radio to X-ray (NED), nonthermal X-ray nuclear emission (Balmaverde et al. 2006), hard X-ray (*Swift*/BAT; reconstructed from Ajello et al. 2009), EGRET upper limit (Reimer et al. 2003), Whipple upper limit (Perkins et al. 2006), and *Fermi* (this work). The RATAN, MOVAVE and MITSuME data are contemporaneous with the *Fermi* data. *Swift* UVOT data come from most recent archival observation in December 2007. The SED is fitted with a one-zone synchrotron/SSC model (blue dashed curve) and a decelerating flow model (Georganopoulos & Kazanas 2003b; blue solid curves). See the text for parameters.

The blue solid curves in Figure 7 represent the SED as seen at an angle $\theta = 20^\circ$ (approximately coincident with $\theta_{\rm jet} \sim 32^\circ$; Asada et al. 2006).[69] Models with structure jets involving decelerating flows, considered here, or a spine-sheath model (Ghisellini et al. 2005), make predictions for FR I radio galaxies as potential *Fermi* γ-ray sources. Indeed, Ghisellini et al. (2005) predicted that 3C 84 would be one of the strongest γ-ray emitting radio galaxies above 100 MeV.

5. CONCLUSIONS

We have reported the discovery that the radio galaxy 3C 84, associated with NGC 1275 is a source of high-energy γ rays in the 100 MeV–GeV range based on data taken with the *Fermi Gamma-ray Space Telescope* between 2008 August and December. The emission is consistent with a point source centered at the nucleus of NGC 1275. No convincing variability is evident in the Fermi data, though there is a hint of a declining flux during the four-month observing period. Compared with the EGRET flux upper limit, however, the γ-ray flux measured with *Fermi* is almost an order-of-magnitude brighter and therefore implies that the NGC 1275 is varying significantly on timescales from months to years. These results limit the amount of flux that can originate from extended galaxy-cluster or dark matter annihilation radiation to the flux upper limit measured with EGRET.

Associated with the γ-ray observations, we also report contemporaneous and historical radio data from 3C 84. The

[69] This was obtained using the brightness ratio of the northern and southern radio lobes, apparent velocity, and apparent distance between the core and jet from recent VLBI observations.

long-term radio light curve appears to be brightening from an historical minimum at 8.0 and 14.5 GHz. Core brightening during the *Fermi* era may be related to its brighter γ-ray flux state than observed with EGRET, but no unambiguous radio/γ-ray flux correlation is evident from the historical data.

Two jet models were used to fit the broadband SED of the nuclear emission from NGC 1275. A simple one-zone SSC model gives an adequate fit to the SED with a moderate Lorentz factor. A decelerating jet model motivated by expectations of larger Lorentz factors in BL Lac/FR 1 unification scenarios also provides a good fit to the data.

During the first year all-sky survey and beyond, we will continue to monitor the flux variations of NGC 1275 and other sources to establish the variability timescale and the fraction of γ-ray emission associated with compact regions. Future monitoring campaigns covering various wavebands of the electromagnetic spectrum will provide crucial data for understanding possible correlations between high- and low-energy bands and discriminating between models. The *Fermi* γ-ray observatory will provide substantial insight into the physics of radio galaxies and clusters in general.

The *Fermi* LAT Collaboration acknowledges generous support from NASA and DOE, the Commissariat à l'Energie Atomique and the Centre National de la Recherche Scientifique/Institut National de Physique Nucléaire et de Physique des Particules in France, the Agenzia Spaziale Italiana and the Istituto Nazionale di Fisica Nucleare in Italy, the Ministry of Education, Culture, Sports, Science and Technology (MEXT), High Energy Accelerator Research Organization (KEK) and Japan Aerospace Exploration Agency (JAXA) in Japan, and the K. A. Wallenberg Foundation, the Swedish Research Council and the Swedish National Space Board in Sweden. Additional support is gratefully acknowledged for science analysis during the operations phase from the Istituto Nazionale di Astrofisica in Italy and the K. A. Wallenberg Foundation in Sweden, which provided a grant in support of a Royal Swedish Academy of Sciences Research fellowship for J.C.

This research made use of the NASA/IPAC Extragalactic Database (NED), which is operated by the Jet Propulsion Laboratory, Caltech, under contact with the National Aeronautics and Space Administration, and data from the University of Michigan Radio Astronomy Observatory, which is supported by the National Science Foundation and by funds from the University of Michigan. The National Radio Astronomy Observatory is a facility of the National Science Foundation operated under cooperative agreement by Associated Universities, Inc. RATAN–600 observations are partly supported by the Russian Foundation for Basic Research (projects 01-02-16812, 05-02-17377, 08-02-00545). The MOJAVE project is supported under National Foundation grant 0807860-AST and NASA-Fermi grant NNX08AV67G.

REFERENCES

Abdo, A., et al. (*Fermi*-LAT Collaboration) 2009, ApJS, in press (arXiv: 0902.1340)
Acciari, V. A., et al. 2009, ApJ, 693, L104
Ajello, M., et al. 2009, ApJ, 690, 367
Albert, J., et al. 2007, ApJ, 666, L17
Aller, H. D., et al. 1985, ApJS, 59, 513
Angel, J. R. P., & Stockman, H. S. 1980, ARA&A, 18, 321
Asada, K., et al. 2006, PASJ, 58, 261
Atoyan, A. M., & Völk, H. J. 2000, ApJ, 535, 45
Atwood, W. B., et al. (*Fermi*-LAT Collaboration) 2009, ApJ, submitted (arXiv:0902.1089)
Baars, J. W. M., et al. 1977, A&A, 61, 99
Balmaverde, B., Capetti, A., & Grandi, P. 2006, A&A, 451, 35
Berezinsky, V. S., Blasi, P., & Ptuskin, V. S. 1997, ApJ, 487, 529
Böhringer, H., Voges, W., Fabian, A. C., Edge, A. C., & Neumann, D. M. 1993, MNRAS, 264, L25
Burns, J. O. 1990, AJ, 99, 14
Cavaliere, A., & Fusco-Femiano, R. 1976, A&A 49, 137, 286, 415
Churazov, E., Forman, W., Jones, C., & Böhringer, H. 2003, ApJ, 590, 225
Ciprini, S., et al. 2008, in Proc. of Science, Workshop on Blazar Variability across the Electromagnetic Spectrum (Trieste: SISSA), PoS (BLAZARS 2008) 072
Colafrancesco, S., Profumo, S., & Ullio, P. 2007, Phys. Rev. D, 75, 023513
Dunn, R. J. H., & Fabian, A. C. 2004, MNRAS, 355, 862
Ettori, S., Fabian, A. C., & White, D. A. 1998, MNRAS, 300, 837
Fabian, A. C., Sanders, J. S., Allen, S. W., Crawford, C. S., Iwasawa, K., Johnstone, R. M., Schmidt, R. W., & Taylor, G. B. 2003, MNRAS, 344, L43
Fabian, A. C., Sanders, J. S., Taylor, G. B., & Allen, S. W. 2005, MNRAS, 360, L20
Fabian, A. C., Sanders, J. S., Taylor, G. B., Allen, S. W., Crawford, C. S., Johnstone, R. M., & Iwasawa, K. 2006, MNRAS, 366, 417
Fabian, A. C., et al. 2000, MNRAS, 318, L65
Fabian, A. C., et al. 2003, MNRAS, 344, L43
Finke, J. D., Dermer, C. D., & Böttcher, M. 2008, ApJ, 686, 181
Fossati, G., Maraschi, L., Celotti, A., Comastri, A., & Ghisellini, G. 1998, MNRAS, 299, 433
Fujita, Y., Kohri, K., Yamazaki, R., & Kino, M. 2007, ApJ, 663, L61
Georganopoulos, M., & Kazanas, D. 2003a, ApJ, 589, L5
Georganopoulos, M., & Kazanas, D. 2003b, ApJ, 594, L27
Ghisellini, G., Tavecchio, F., & Chiaberge, M. 2005, A&A, 432, 401
Hartman, R. C., Kadler, M., & Tueller, J. 2008, ApJ, 688, 852
Hartman, R. C., et al. 1999, ApJS, 123, 79
Kataoka, J., et al. 2006, ApJ, 641, 158
Kellermann, K. I., et al. 2004, ApJ, 609, 539
Kotani, T., et al. 2005, II Nuovo Cimento C, 28, 755
Kovalev, Y. Y., Nizhelsky, N. A., Kovalev, Y. A., Berlin, A. B., Zhekanis, G. V., Mingaliev, M. G., & Bogdantsov, A. V. 1999, A&AS, 139, 545
Kubo, H., et al. 1998, ApJ, 504, 693
Laing, R. A., & Bridle, A. H. 2002, MNRAS, 336, 328
Lister, M. L., et al. 2009, AJ, 137, 3718
Mayer-Hasselwander, H. A., et al. 1982, A&A, 105, 164
Molendi, S., & Gastaldello, F. 2009, A&A, 493, 13
Mukherjee, R., Halpern, J., Mirabal, N., & Gotthelf, E. V. 2002, ApJ, 574, 693
Nandikotkur, G., et al. 2007, ApJ, 657, 706
Nesterov, N. S., Lyuty, V. M., & Valtaoja, E. 1995, A&A, 296, 628
Nevalainen, J., Oosterbroek, T., Bonamente, M., & Colafrancesco, S. 2004, ApJ, 608, 166
Nilsson, K., et al. 2007, A&A, 475, 19
O'Dea, C. P., Dent, W. A., & Balonek, T. J. 1984, ApJ, 278, 89
Osako, C. Y., et al. 1994, ApJ, 435, 181
Perkins, J. S., et al. 2006, ApJ, 644, 148
Piner, B. G., Pant, N., & Edwards, P. G. 2008, ApJ, 678, 64
Primini, F. A., et al. 1981, ApJ, 243, L13
Pronik, I. I., Merkulova, N. I., & Metik, L. P. 1999, A&A, 351, 21
Reimer, O., Pohl, M., Sreekumar, P., & Mattox, J. R. 2003, ApJ, 588, 155
Roming, P. W. A., et al. 2005, Space Sci. Rev., 120, 95
Sanders, J. S., & Fabian, A. C. 2007, MNRAS, 381, 1381
Sanders, J. S., Fabian, A. C., & Dunn, R. J. H. 2005, MNRAS, 366, 133
Sreekumar, P., et al. 1998, ApJ, 494, 523
Sreekumar, P., Bertsch, D. L., Hartman, R. C., Nolan, P. L., & Thompson, D. J. 1999, Astropart. Phys., 11, 221
Strong, A. W., & Bignami, G. F. 1983, ApJ, 274, 549
Strong, A. W., et al. 1982, A&A, 115, 404
Taylor, G. B., Gugliucci, N. E., Fabian, A. C., Sanders, J. S., Gentile, G., & Allen, S. W. 2006, MNRAS, 368, 1500
Taylor, G. B., & Vermeulen, R. C. 1996, ApJ, 457, L69
Teräsranta, H., et al. 2004, A&A, 427, 769
Totani, T. 2004, Phys. Rev. Lett., 92, 1301
Totani, T., & Kitayama, T. 2000, ApJ, 545, 572
Vermeulen, R. C., Readhead, A. C. S., & Backer, D. C. 1994, ApJ, 430, L41
Veron-Cetty, M.-P., & Veron, P. 1998, Scientific Report of ESO, No. 18
Walker, R. C., Dhawan, V., Romney, J. D., Kellermann, K. I., & Vermeulen, R. C. 2000, ApJ, 530, 233
Walker, R. C., Romney, J. D., & Benson, J. M. 1994, ApJ, 430, L45